JOURNAL OF Materials CHEMISTRY

Overcoming Jahn–Teller distortion of oxysulfide spinel materials for lithium secondary batteries

Yang-Kook Sun* and Yang-Seok Jeon

Electrochemistry Laboratory, Samsung Advanced Institute of Technology, 103-6, Moonji-Dong, Yusong-Gu, Daejon, Korea, 305-380. E-mail: yksun@sait.samsung.co.kr

Received 23rd August 1999, Accepted 20th October 1999

A new sulfur-doped spinel material, $LiAl_{0.24}Mn_{1.76}O_{3.98}S_{0.02}$ with submicron dimensions and well developed octahedron morphology is synthesized by a sol–gel method using glycolic acid as a chelating agent. $LiAl_{0.24}Mn_{1.76}O_{3.98}S_{0.02}$ electrodes cycled in various voltage regions were characterized by means of charge–discharge experiments and XRD to investigate their structural integrity. The material overcomes Jahn–Teller distortion in all voltage operating regions. Our synthesized material shows excellent cyclability and delivers capacities of 215 mA h g^{-1} over the 3 and 4 V regions (4.3–2.4 V).

Introduction

Presently commercialized lithium-ion batteries use layer structured $LiCoO_2$ cathodes. Although $LiCoO_2$ cathodes exhibit excellent performance characteristics, an intensive search for new cathode materials has been carried out for many years because of the high cost and toxicity of $LiCoO_2$. One of the most attractive cathode materials is the spinel $LiMn_2O_4$ and its derivatives.[1–4] $Li_xMn_2O_4$ ($x=1$) has a cubic spinel structure with space group symmetry *Fd*3*m* in which the Li^+ and $Mn^{3+/4+}$ ions are located on the 8a tetrahedral sites and the 16d octahedral sites, respectively.[5,6] Lithium extraction from the 8a tetrahedral sites in $Li_xMn_2O_4$ (*i.e.* for $0 \leqslant x \leqslant 1$) occurs at 4 V *vs.* metallic lithium. It seems that the cubic structure of the material is maintained during the extraction and insertion of lithium ions at this voltage, but that the capacity of the electrode slowly fades during the process. Although some reasons for the capacity loss of 4 V Li/$Li_xMn_2O_4$ cells has been proposed, the origin of the fading has not, as yet, been clearly understood.[3,7–9] Recently, Thackeray *et al.* suggested that the dissolution of a Mn^{3+}-rich $Li_2Mn_2O_4$ phase formed on the surface of the particles at the end of discharge (above 3 V) might contribute to capacity loss in the 4 V region.[10]

For $1 \leqslant x \leqslant 2$, it has been reported that lithium ions are inserted into the empty 16c octahedral sites of the spinel structure at *ca.* 3 V.[5,6] Lithium insertion into $LiMn_2O_4$ results in the transition of the structure from cubic into tetragonal $Li_2Mn_2O_4$, which is accompanied by a Jahn–Teller distortion owing to the reduction of the average oxidation state of Mn from 3.5 to 3.0. The increased concentration of Mn^{3+} ions in the host structure reduces the crystal symmetry from cubic ($c/a=1$) to tetragonal ($c/a=1.16$).[6] This structural distortion is too large for the spinel framework to withstand its structural integrity during the cycling. This explains why the cubic spinel $LiMn_2O_4$ is more stable in cyclability in the 4 V region than in the 3 V region and is limited to use only for 4 V electrodes.

Here we report the synthesis and electrochemical performance of a new sulfur-doped spinel material, $LiAl_{0.24}Mn_{1.76}O_{3.98}S_{0.02}$, which overcomes the Jahn–Teller distortion. XRD was carried out to investigate the structural integrity of the oxysulfide host.

Experimental

$LiAl_{0.24}Mn_{1.76}O_{3.98}S_{0.02}$ powders were prepared by a sol–gel method using glycolic acid as a chelating agent according to the process shown in Fig. 1. $Li(CH_3COO)\cdot 2H_2O$, $Mn(CH_3COO)_2\cdot 4H_2O$, Li_2S and $Al(NO_3)_3\cdot 9H_2O$ (cationic ratio of Li : Mn : Li : Al = 0.75 : 1.75 : 0.3 : 0.25) were dissolved in distilled water, and added dropwise to a continuously stirred aqueous solution of glycolic acid. The pH of the solution was adjusted to 8.5–9.5 using ammonium hydroxide. The resultant solution was evaporated at 70–80 °C until a transparent sol and gel was obtained. The resulting gel precursors were decomposed at 500 °C for 10 h in air and the decomposed powders were calcined at 800 °C in air for 10 h and then in flowing oxygen for 15 h.

Powder X-ray diffraction (Rigaku, Rint-2000) using Cu-Kα

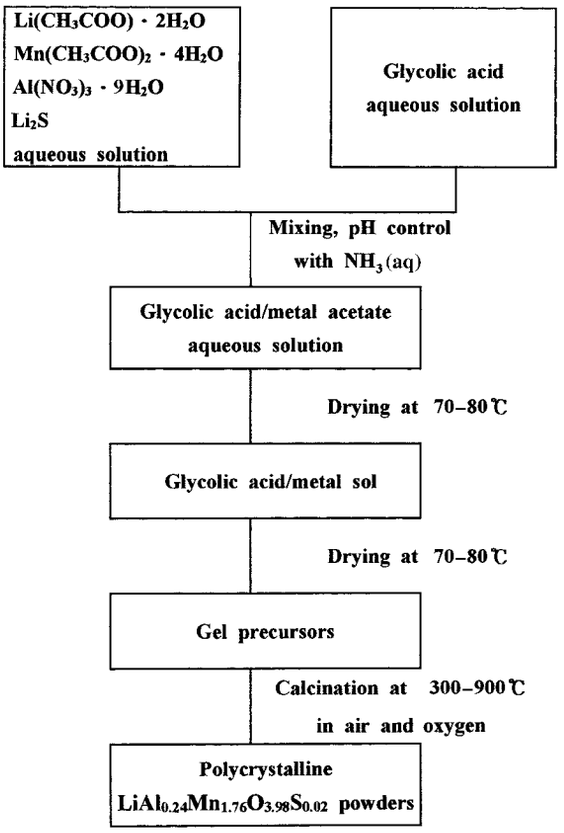

Fig. 1 Flowchart of the procedure to prepare polycrystalline $LiAl_{0.24}Mn_{1.76}O_{3.98}S_{0.02}$ powders by a sol–gel method.

radiation was used to identify the crystalline phase of the materials. Rietveld refinement was then performed on the X-ray diffraction data to obtain the lattice constants. The composition of the powders was measured by inductively coupled plasma (ICP) spectroscopy after dissolving the powders in dilute nitric acid. Sulfur was analyzed with a sulfur analyzer (LECO Co., CS 444) and oxygen content was determined from the mass balance. The morphology of the particles was observed using a field emission scanning electron microscope (FE-SEM) (Hitachi Co., S-4100).

For the fabrication of the electrodes, the $LiAl_{0.24}Mn_{1.76}O_{3.98}S_{0.02}$ powders were mixed with 12 wt% carbon black and 8 wt% poly(tetrafluoroethylene) (PTFE), with the mixture pressed onto aluminium exmet. Lithium foil was used as the anode. The electrolyte was a 1 : 1 v/v mixture of ethylene carbonate (EC) and propylene carbonate (PC) containing 1 M $LiClO_4$. Charge–discharge cycles were performed galvanostatically at a current density of 0.2 mA cm^{-2}.

Results and discussion

The as-prepared powders were confirmed to have a well defined spinel phase structure with space group *Fd3m*, as shown by X-ray diffraction (XRD). The lattice constant of the powders was 8.191 Å which is lower than that of the stoichiometric spinel $LiMn_2O_4$ (8.245 Å) or $Li_{1.03}Mn_2O_4$ (8.225 Å).[7,11] Previous reports revealed that the lattice constant of metal-doped $LiM_xMn_{2-x}O_4$ spinel structures decrease with the amount of doped metal owing to an increasing concentration of Mn^{4+} ions in the spinel structure by substituting Mn^{3+} ions by metal ions.[12,13] Chemical analysis data show the sample to have stoichiometry $LiAl_{0.24}Mn_{1.76}O_{3.98}S_{0.02}$.

Fig. 2 shows a scanning electron micrograph (SEM) of a prepared powder. The morphology of the particles is analogous to that of single crystals of gold with cubic structure. The particles are shaped into well developed polyhedra of mainly octahedral configuration bounded by eight (111) planes. They are quite different in particle morphology from the stoichiometric spinel which has a well developed (100) plane. The average diameter of the particles was *ca.* 1 μm.

Fig. 3 shows charge–discharge curves measured at a constant current density of 0.2 mA cm^{-2} in three different voltage regions as a function of cycle number. Fig. 3(a) shows that the charge–discharge curves measured in the voltage range 4.4–3.0 V have only one plateau. This is quite a different result from that observed for the stoichiometric spinel $LiMn_2O_4$.[7,14,15] The initial capacity of the material delivers 99 mA h g^{-1} in the range 4.4–3.0 V which is somewhat lower than that of the stoichiometric spinel $LiMn_2O_4$. The discharge capacity slowly increases during cycling and remains at 105 mA h g^{-1} at the 35th cycle and the material shows excellent cyclability without any capacity loss even after the 35th cycle. The electrochemical cyclability of the material was examined in the 3 V region since most capacity loss of the stoichiometric spinel $LiMn_2O_4$ occurs at this voltage range. The cell was first discharged down to 2.4 V and then cycled between the voltage range 3.5–2.4 V. It has been reported that the voltage plateau appearing at *ca.* 2.85 V for $LiMn_2O_4$ is mainly due to the intercalation of Li ions into cubic $LiMn_2O_4$ to form tetragonal $Li_2Mn_2O_4$.[3,5,6] The $LiAl_{0.24}Mn_{1.76}O_{3.98}S_{0.02}$ electrode initially delivers a discharge capacity of 96 mA h g^{-1}, which on cycling gradually increases to reach 123 mA h g^{-1} after the 35th cycle, as shown in Fig. 3(b). It is also interesting that the polarization (half of the voltage difference between the charge and discharge curves) decreases with cycling, indicative of an improved cyclability of the electrode. The discharge–charge behavior of the material is a unique feature in contrast to those of the spinel $LiMn_2O_4$ and its derivatives,[2,15,16] which show a rapid capacity loss during cycling at this voltage region. Fig. 3(c) shows the charge–discharge curves for a $Li/LiAl_{0.24}Mn_{1.76}O_{3.98}S_{0.02}$ cell in the voltage range 4.3–2.4 V, encompassing both the 4 and 3 V plateaus. The cell was first charged up to 4.3 V and repeatedly cycled in the voltage range between 2.4 and 4.3 V. The discharge capacity in the 3 V region rapidly increases up to the third cycle and subsequently stabilizes upon further cycling. The capacity at the 4 V region remains almost constant with cycling. The total capacity of the material over both the 3 and 4 V regions increases from 201 mA h g^{-1} for the first cycle to 215 mA h g^{-1} for the 30th cycle as a result of an increase of capacity in the 3 V region.

It is inferred from the above results that the oxysulfide spinel possesses a more flexible structure than the spinel $LiMn_2O_4$ and its derivatives, so preventing a transition from a cubic to a tetragonal phase. In a previous report,[17] we studied the effect of Al substitution for Mn ($LiAl_{0.24}Mn_{1.76}O_4$) and S for O ($LiMn_2O_{3.98}S_{0.02}$) in $LiMn_2O_4$ on the electrochemical cyclability. Whereas the electrochemical cyclability of $LiAl_{0.24}Mn_{1.76}O_4$ in the 3 V region decreases rapidly, the discharge capacity of the $LiMn_2O_{3.98}S_{0.02}$ electrode in the 3 V region initially delivers 80 mA h g^{-1}, and steadily increases during cycling. Goodenough reported that for the thiospinel

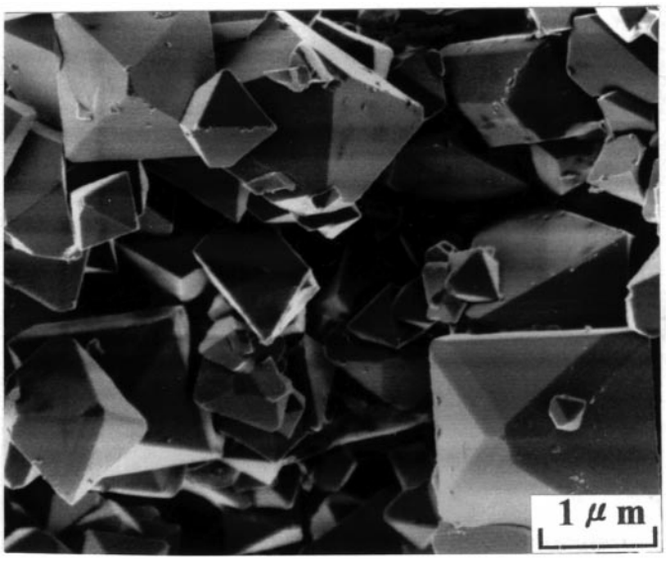

Fig. 2 Scanning electron micrograph of a $LiAl_{0.24}Mn_{1.76}O_{3.98}S_{0.02}$ sample.

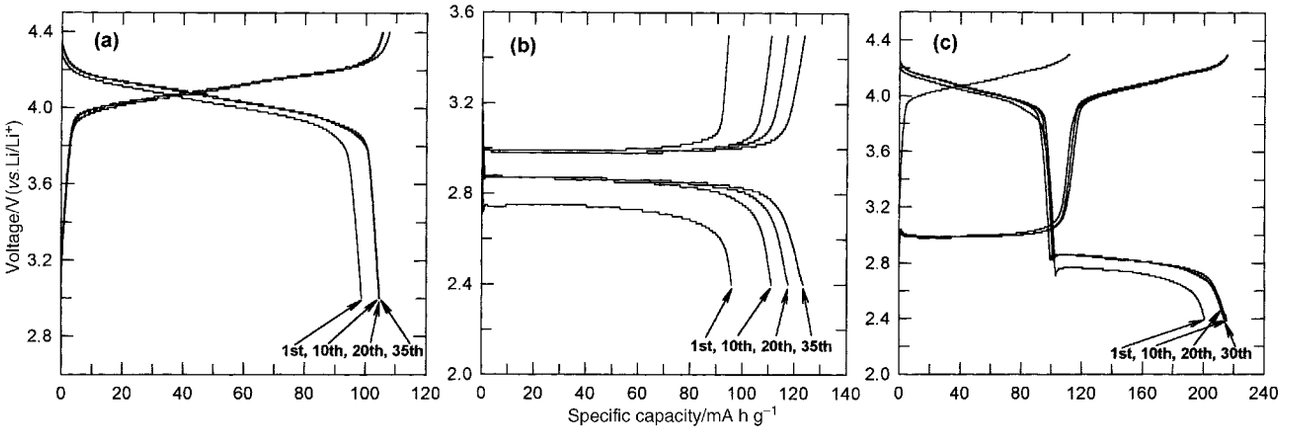

Fig. 3 Cycling charge–discharge curves for the $LiAl_{0.24}Mn_{1.76}O_{3.98}S_{0.02}$/Li cell in the voltage ranges (a) 4.4–3.0, (b) 2.4–3.5 and (c) 4.3–2.4 V.

($Li_xTi_2S_4$) structure, the octahedral site preference of the Li^+ ion is strong enough to overcome the electrostatic interactions favoring tetrahedral site occupancy, so that Li^+ ions move into interstitial 16c octahedral sites as in the layered Li_xTiS_2 structure.[18] He also proposed that the relatively large size and polarizability of the sulfide ions allow 3D Li^+-ion transport between edge-shared octahedral sites to be just as facile in $Li_xTi_2S_4$ as is 2D Li^+-ion transport in Li_xTiS_2. Therefore, we speculate that the substitution of a small amount S for O not only stabilizes the structural integrity of the electrode at 3 V range but also increases the Li^+ ion transport in the electrode, which in turn increases the electrochemical performance. From the above results, we conclude that the elimination of the Jahn–Teller distortion of $LiAl_{0.24}Mn_{1.76}O_{3.98}S_{0.02}$ in the 3 V region is attributed to S substitution for O.

Although the oxysulfide exhibits a larger voltage drop between the 4 and 3 V plateau, it delivers a large capacity of 215 mA h g^{-1}, corresponding to an energy density of 702 W h kg^{-1}, that is higher than those of $LiCoO_2$ (518 W h kg^{-1}) and $LiNi_{0.85}Co_{0.15}O_2$ (675 W h kg^{-1}). This indicates that our synthesized oxysulfide spinel material can be used as a potential cathode for lithium secondary batteries.

It is well known that the cyclability of lithium secondary batteries depends greatly on the structural integrity of the host materials during charge and discharge.[19] We believe that the excellent capacity retention of the materials both in the 3 and 4 V regions may be associated with the stability of the spinel structure. In order to investigate the structural change of the electrode during cycling, the electrode was characterized by XRD before and after cycling.

Fig. 4 shows X-ray diffraction patterns for the as-prepared powders and electrodes cycled in the 4 V region, the 3 V region, and both regions. The Li/$LiAl_{0.24}Mn_{1.76}O_{3.98}S_{0.02}$ cell was allowed to equilibrate for 5 h in the fully discharged state. The cell was disassembled, the $LiAl_{0.24}Mn_{1.76}O_{3.98}S_{0.02}$ electrode removed from the cell and dried for one day. When comparing XRD patterns of the cycled electrodes at various voltage regions [Fig. 4(b)–(d)] with that of as-prepared powders [Fig. 4(a)], we are unable to find any difference in the position of the characteristic peaks for the typical spinel phase structure although there was some variation of peak intensities. Considering the variation of the levels of preferential orientation in preparing the samples, it is reasonable to state that there is almost no difference in the peak intensities of the cycled electrodes. These observations clearly show that our synthesized oxysulfide spinel cathode retains its original cubic spinel phase at all the operating voltage regions, indicating overcoming of the Jahn–Teller distortion in the spinel Mn phase.

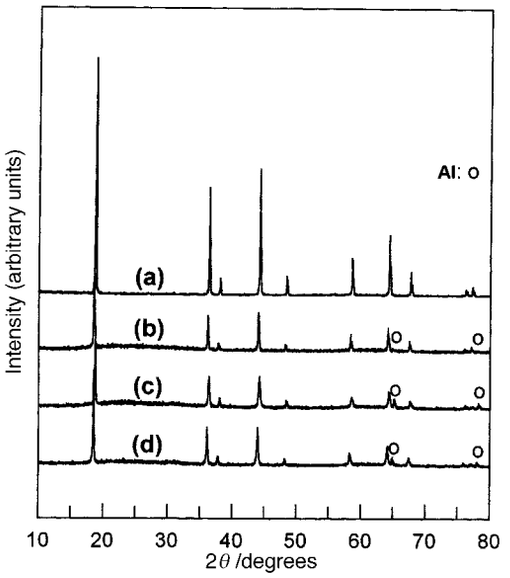

Fig. 4 X-Ray diffraction patterns for (a) $LiAl_{0.24}Mn_{1.76}O_{3.98}S_{0.02}$ and $LiAl_{0.24}Mn_{1.76}O_{3.98}S_{0.02}$ electrodes cycled in the voltage ranges (b) 4.4–3.0, (c) 2.4–3.5 and (d) 4.3–2.4 V.

Conclusions

A new sulfur-doped spinel material, $LiAl_{0.24}Mn_{1.76}O_{3.98}S_{0.02}$, with submicron dimensions and displaying well developed octahedra is synthesized by a sol–gel method using glycolic acid as a chelating agent. The structural integrity of the oxysulfide material as-prepared and after charge–discharge cycling was investigated intensively by XRD. The material shows capacities of 105, 124 and 215 mA h g^{-1} in the 4 V (4.4–3.0 V), 3 V (2.4–3.5 V), and both regions (4.3–2.4 V), respectively, with excellent cyclability. Furthermore, our synthesized material overcomes Jahn–Teller distortion in all voltage operating regions. The preparation of the oxysulfide is a strategy to develop new cathode active materials combining the characteristics of both oxides and sulfides for lithium secondary batteries.

References

1 T. Ohzuku, M. Kitagawa and T. Hirai, *J. Electrochem. Soc.*, 1990, **137**, 769.
2 J. M. Tarascon, E. Wang, F. K. Shokooki, W. R. McKinnon and S. Colson, *J. Electrochem. Soc.*, 1990, **138**, 2858.
3 R. J. Gummow, A. de Kock and M. M. Thackeray, *Solid State Ionics*, 1994, **69**, 59.

4 K. Amine, H. Tukamoto, H. Yasuda and Y. A. Fujita, *J. Electrochem. Soc.*, 1996, **143**, 1607.
5 M. M. Thackeray, W. I. F. David, P. G. Bruce and J. B. Goodenough, *Mater. Res. Bull.*, 1983, **18**, 461.
6 M. M. Thackeray, *Prog. Solid State Chem.*, 1997, **25**, 1.
7 D. H. Jang, Y. J. Shin and S. M. Oh, *J. Electrochem. Soc.*, 1996, **143**, 2204.
8 Y. Xia, Y. Zhou and M. Yoshio, *J. Electrochem. Soc.*, 1997, **144**, 2593.
9 A. Blar, C. Sigala, G. Amatucci, D. Guyomard, Y. Chabre and J. M. Tarascon, *J. Electrochem. Soc.*, 1998, **145**, 194.
10 M. M. Thackeray, Y. Shao-Horn, A. J. Kahaian, K. D. Kepler, E. Skinner, J. Vaughey and S. A. Hackney, *Electrochem. Solid-State Lett.*, 1998, **1**, 7.
11 Y.-K. Sun, *Solid State Ionics*, 1997, **100**, 115.
12 Y.-K. Sun and S.-H. Jin, *J. Mater. Chem.*, 1998, **8**, 2399.
13 Y. E. Eli, W. F. Howard, Jr., S. H. Lu, S. Mukerjee, J. McBreen, J. T. Vaughey and M. M. Thackeray, *J. Electrochem.. Soc.*, 1998, **145**, 1238.
14 Y.-K. Sun, I.-H. Oh and K.-Y. Kim, *Ind. Eng. Chem. Res.*, 1997, **36**, 4839.
15 Z. Jiang and K. M. Abraham, *J. Electrochem. Soc.*, 1996, **143**, 1591.
16 M. M. Thackeray, A. de. Kock, M. H. Rossouw, D. Liles, R. Bittihn and D. Hoge, *J. Electrochem. Soc.*, 1992, **139**, 363.
17 Y.-K. Sun and Y.-S. Jeon, *Electrochem. Commun.*, 1999, **1**, 597.
18 J. B. Goodenough, *Solid State Ionics*, 1994, **19**, 184.
19 M. M. Thackeray, *J. Electrochem. Soc.*, 1995, **142**, 2558.

Paper 9/06811B